Investigation of the co-crystallisation of N-heterocycles

By

Leigh-Anne Loots

Thesis presented in partial fulfilment of the requirements for the degree of Master of Science

at

Stellenbosch University

Department of Chemistry and Polymer Science

Faculty of Science

Supervisor: Leonard J. Barbour

March 2009

4.2.2 O3BN23 – Resorcinol and phthalazine

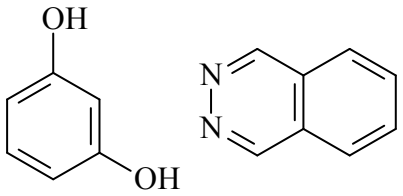

Scheme 4.3 Co-crystal formers resorcinol and phthalazine.

Single-crystals of O3BN23 have yet to be obtained for SCD analysis. Only a limited number of solvent systems have been tested thus far, yielding no suitable single crystals. The 3-D structure of O3BN23 is therefore not discussed here.

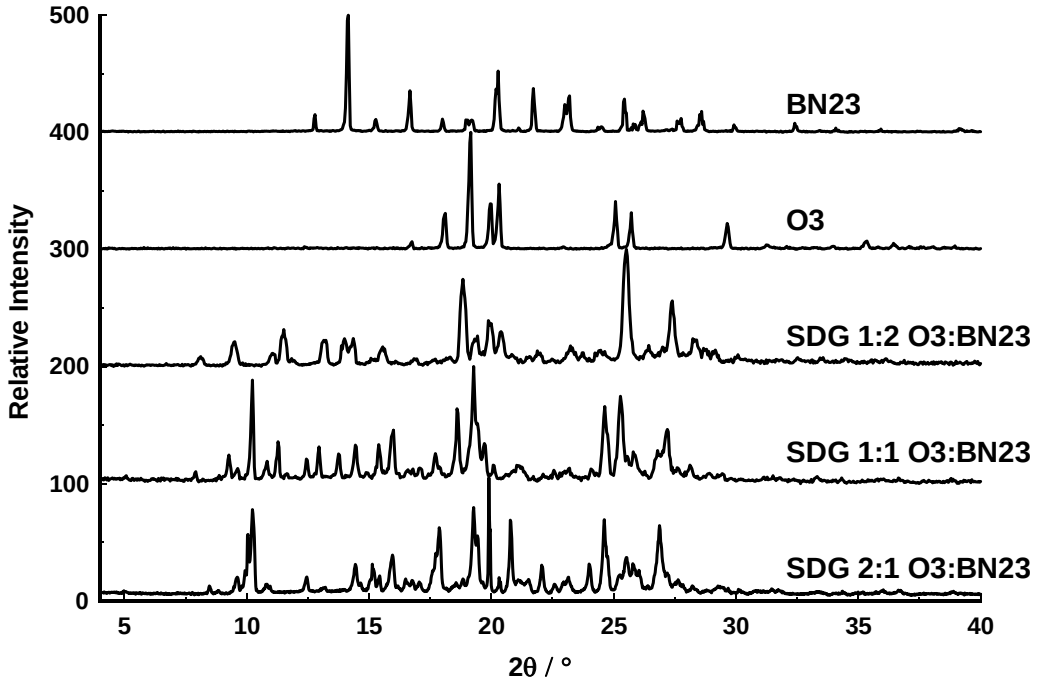

Figure 4.15 Comparison of PXRD results of SDG experiments with the starting materials resorcinol and phthalazine.

Solvent-drop grinding experiments, performed with three different molar ratios of starting material, yielded two distinct products as evidenced by PXRD analysis. From the powder diffractograms obtained it is clear that all three products obtained are noticeably different from the starting materials (Figure 4.15) and reasonably different from one another. The 1:2 and 2:1 products can easily be distinguished from one another, while the equimolar product appears to be a mixture of these two forms. These results infer the formation of two new co-crystals. The DSC analysis (Figure 4.16) of the 1:1 and 2:1 products exhibit similar thermal behaviour, both producing thermal events at 98 °C. The form containing excess resorcinol has a second, smaller thermal event at 70 °C that could be due to a rearrangement and not a

melt. The thermal trace of the 1:2 composition comprises a single event that corresponds to the melting of the co-crystal (onset at 74 °C). The 1:1 form does not exhibit this same peak to verify a mixture of forms, however, this may mean that the one form constitutes the majority of the sample.

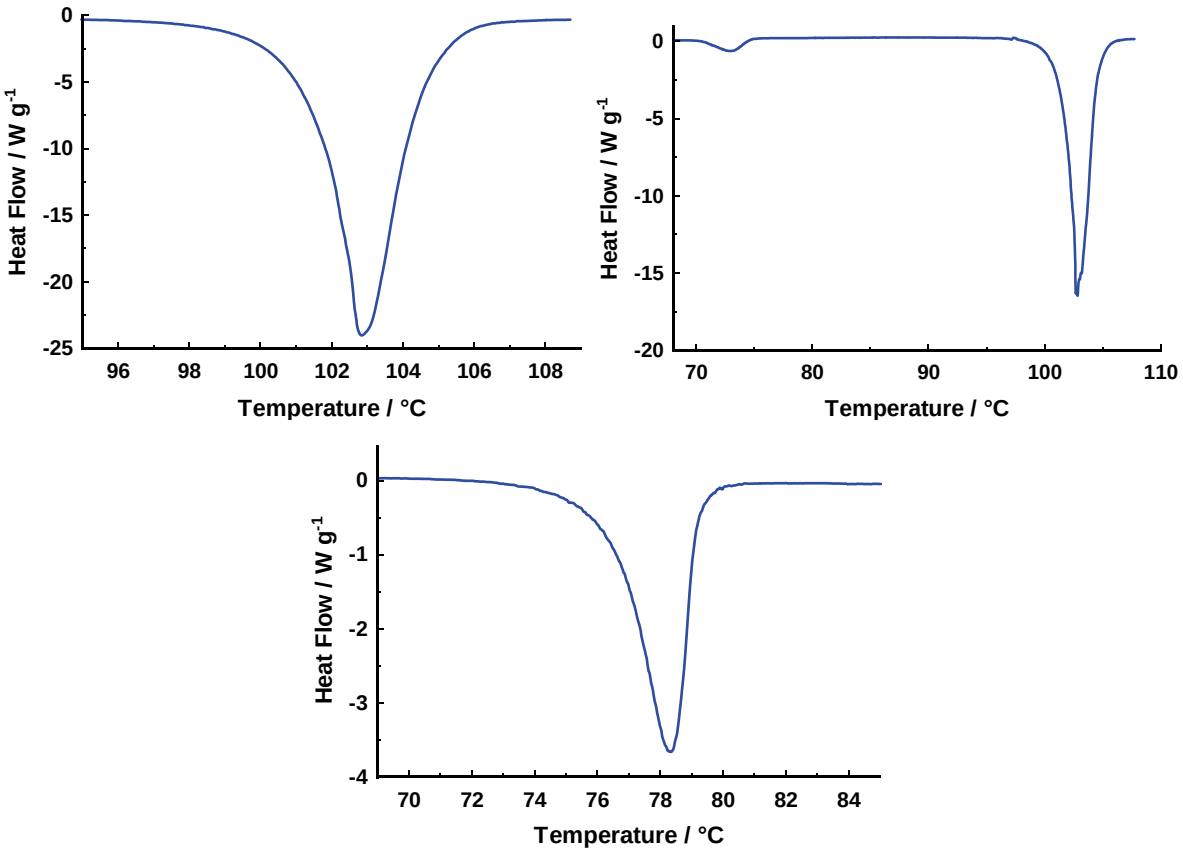

Figure 4.16 DSC trace of the 1:1 (top left), 2:1 (top right) and 1:2 (bottom) SDG products of O3BN23.

Without single-crystal structures corresponding to the PXRD data, it is difficult to determine if the products are in fact co-crystals, although the PXRD and DSC results are promising. The PXRD and DSC data may infer that novel co-crystals are formed by solvent-drop grinding, however these analytical techniques do not provide information regarding the intermolecular interactions of the structure. Single-crystal diffraction is the only means with which to unambiguously elucidate this information.

4.2.3 O4BN23 – Hydroquinone and phthalazine (2:4)

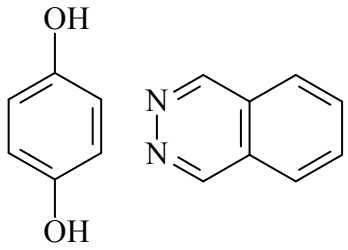

Scheme 4.4 Co-crystal formers hydroquinone and phthalazine.

The structure of O4BN23 was refined in the lowest symmetry space group, *P*1, with two hydroquinone molecules and four phthalazine molecules in the ASU (Figure 4.17). Hydroquinone molecules each hydrogen bond to two phthalazine molecules to form ternary adducts. The number of molecules in the ASU, and similar arrangement of the two adducts, suggests the possibility of incorrect space group assignment. However, structure solution and refinement attempted in the higher symmetry space group, $P\bar{1}$, yields an unsatisfactory model. Non-crystallographic inversion centres (red circle in the figure) are located between molecules **A** and **B**. This inversion centre imposes *pseudosymmetry* on the structure and verifies that *P*1 is the correct space group choice.

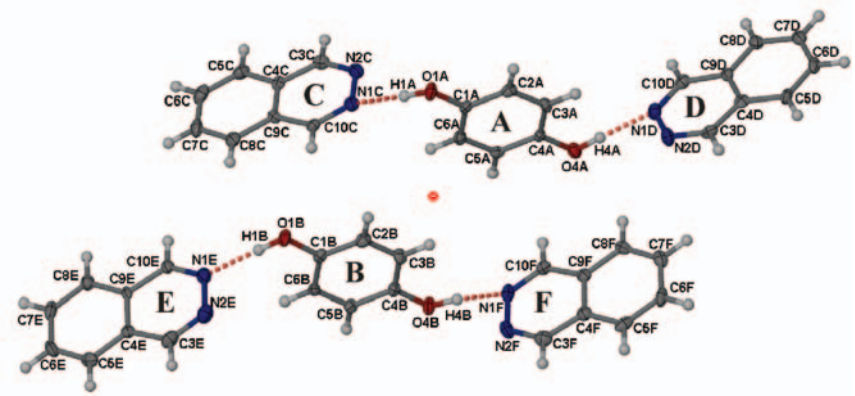

Figure 4.17 Thermal ellipsoid plot of the ASU of O4BN23. Inversion centre is indicated by red circle.

Viewing the structure along [100] it is quite apparent that the molecules are symmetry–independent owing to a slight difference in hydrogen bonding patterns of the two ternary adducts (Figure 4.18). In the adduct labelled **1** hydrogen bonds form on the same side of the phthalazine molecules such that the "unused" N–atoms are both oriented in a common direction. This is similar to the effect of a mirror plane bisecting the hydroquinone of adduct **1**. In adduct **2**, however, the unused N–atoms are directed to either side of the hydroquinone ring. This is similar to a 2-fold rotation axis running through hydroquinone of adduct **2**,

parallel to the *a* axis. If we consider the possibility of adduct **2** forming a hydrogen bond to the N–atom at the top (Figure 4.18), then the hydroxyl hydrogen atom would either have to project out of the plane of the aromatic ring or the entire O4 ring would have to move. It has been observed that the hydroxyl group prefers to remain in the plane of the ring, and movement of the ring would involve very close interactions with neighbouring phthalazine rings. Both of these scenarios are considered unfavourable in this instance.

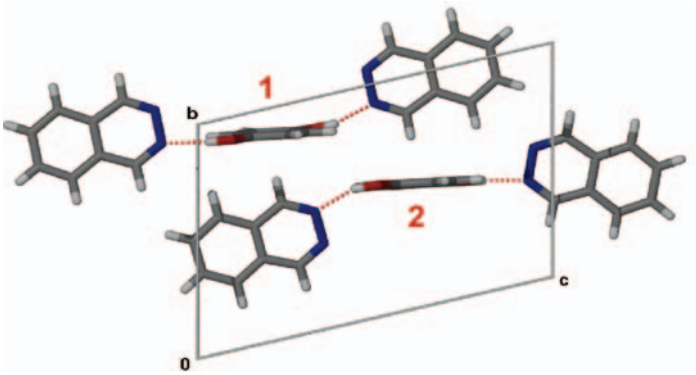

Figure 4.18 The ASU of O4BN23 viewed along [100] reveals the difference between the two adducts – in one adduct the O–H⋯N bonds are on the same side of the phthalazine molecules so that the "unused" N–atoms are orientated towards the same direction, whilst in the other adduct the "unused" N atoms are not facing a common direction.

The fingerprint plot of O4BN23 (Figure 4.19) illustrates a similar pattern to that observed for O2BN23 (Figure 4.9). Both plots feature significant π⋯π interactions between adjacent phthalazine rings, indicated by the yellow-green area on the diagonal (1.8 Å) for O4BN23. Further evidence of the similarity between the structures of O2BN23 and O4BN23 is observed in Figure 4.20 where it can be seen that phthalazine molecules of O4BN23 stack in a similar fashion to those in O2BN23. Analogous to the structure of O2BN23, the offset π⋯π stacking of the ternary adducts results in weakly associated adduct strings. Alternate strings of O4BN23 show a slipped overlap of phthalazine molecules. A reasonable explanation for the choice of one N–atom over the other equally accessible N–atom on phthalazine molecules from which to form hydrogen bonds cannot be formulated.

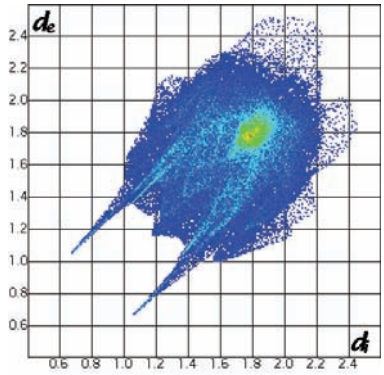

Figure 4.19 Fingerprint plot of co-crystal O4BN23

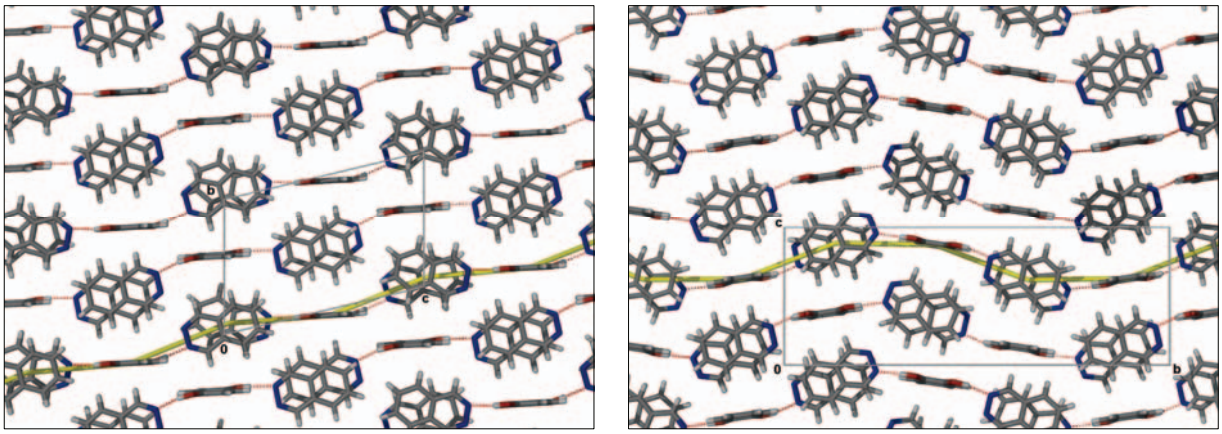

Figure 4.20 Packing diagrams of O4BN23 (left) and O2BN23 (right), showing similar chain formation when both structures are viewed along [100]. Phthalazine molecules in O4BN23 overlap in two different orientations due to different hydrogen bond orientations in symmetry independent adducts.

The structures of O4BN23 and O2BN23 show closely related packing patterns much like the similarities found between *β*–O2N2 and *β*–O4N2 (Chapter 3). It was expected that there would be closer similarities between the related diazine and benzodiazine co-crystals owing to similarities in chemical behaviour. This result implies that the π⋯π interactions between the phthalazine are a driving force in the packing arrangement of these co-crystals.

Single-crystal data were used to simulate a powder diffractogram for comparison with experimental data. Three molar ratios were used in SDG experiments. The simulated diffractogram is comparable to the experimental pattern of the SDG product containing excess phthalazine (Figure 4.21). DSC analysis of this co-crystal shows a single thermal event at approximately 152 °C, representing the co-crystal melting (Figure 4.22). A second, distinct co-crystal form results when hydroquinone is used in excess. DSC analysis of this compound verifies the PXRD results with a single thermal event (onset at 110 °C) that does not correspond to either of the starting materials (hydroquinone 172 °C; phthalazine 89 °C). The single-crystal structure of this co-crystal form has not yet been elucidated. The third diffractogram (1:1) in this comparative study is once more a mixture of the two co-crystal forms. The DSC trace of this product (1:1) verifies the mixture of the two co-crystal forms with two thermal events observed. The first event occurs at approximately 110 °C followed by the second at approximately 150 °C. These two thermal events correlate to those observed in the DSC trace of the individual co-crystal forms.

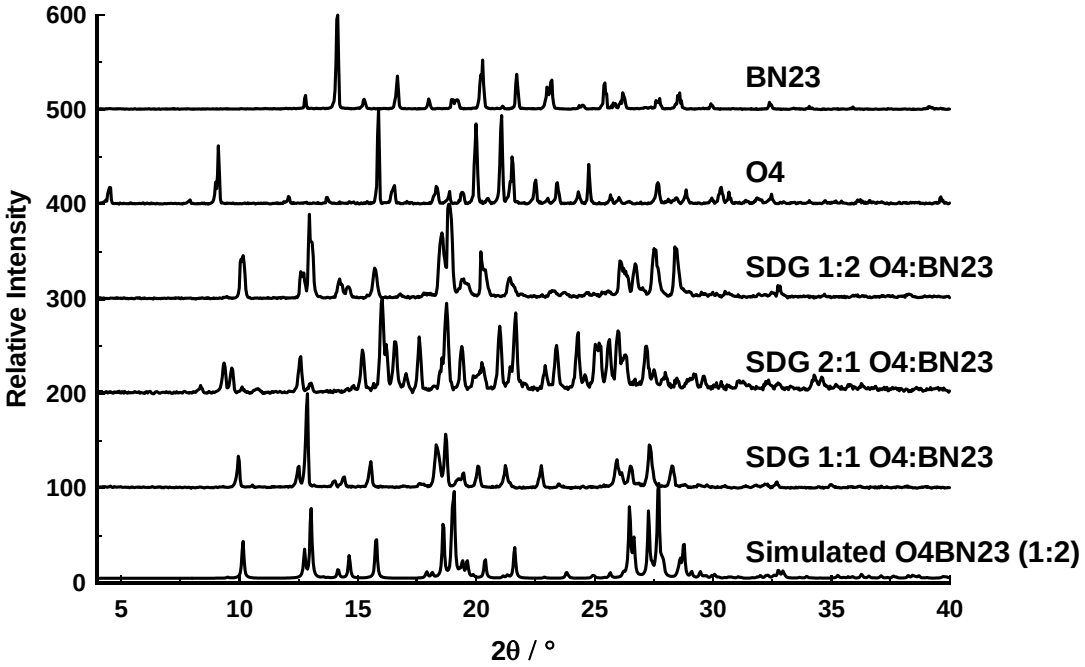

Figure 4.21 PXRD comparison of three separate SDG experiments, utilizing different molar ratios of hydroquinone and phthalazine, with the simulated pattern of O4BN23.

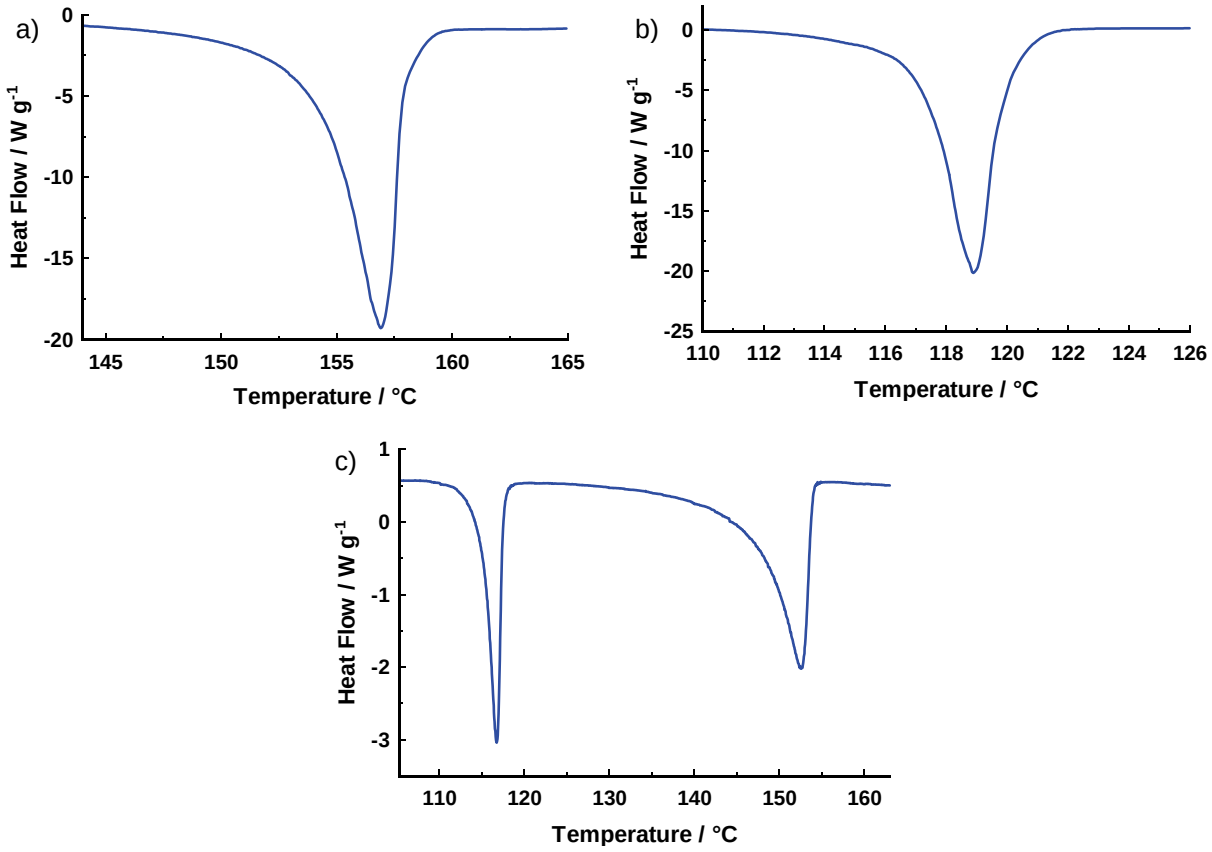

Figure 4.22 DSC trace of a) 1:2, b) 2:1 and c) 1:1 SDG products of O4BN23.

4.2.4 O2BN3 – Catechol and Quinazoline (1:1)

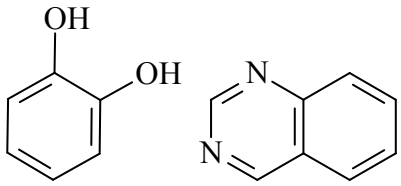

Scheme 4.5 Co-crystal formers catechol and quinazoline.

The ASU of co-crystal O2BN3 consists of a molecule each of catechol and quinazoline, in the monoclinic space group, $P2_1/c$ (Figure 4.23). A fingerprint plot (Figure 4.24) of the co-crystal denotes the presence of short O–H⋯N interactions (longer tails) as well as C–H⋯π interactions (characteristic 'wings'). The C–H⋯π interactions appear more significant than π⋯π interactions in this structure since the area of the plot indicating C⋯C interactions is not as intensely coloured (red-yellow-green) as when stacking interactions are prominent contributors to the stabilisation of the network.

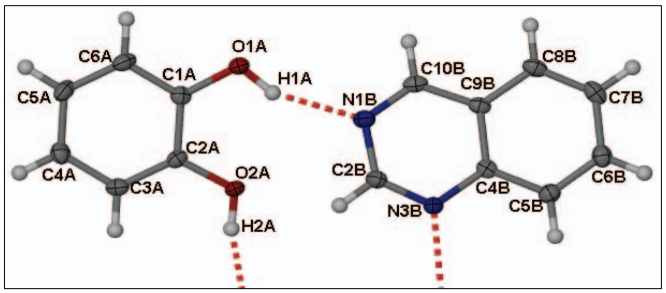

Figure 4.23 Thermal ellipsoid plot of ASU of O2BN3 comprising one molecule each of catechol and quinazoline

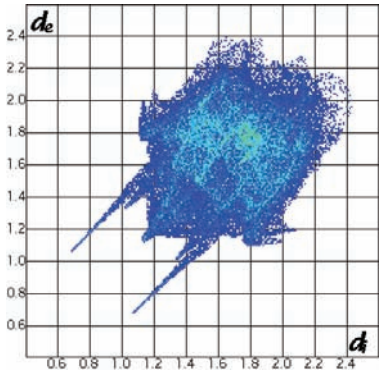

Figure 4.24 Fingerprint plot of O2BN3

The two molecules of the ASU, as depicted in Figure 4.23, hydrogen bond in a 1:1 molar ratio to form a 1-D tape, $C_2^2(10)$, that resembles an over-stretched helix (Figure 4.25). When compared to O2N3 (Chapter 3, section 3.2.4), it is clear that the smaller size of the pyridazine ring plays a part in forming discrete hydrogen bonded rings while in the structure of O2BN3 the molecules arrange themselves into hydrogen bonded tapes to accommodate the increased dimensions of the quinazoline molecule. However, similar features are evident between the two structures O2N3 and O2BN3. The hydrogen bonding network of the two structures is not the same, however; when viewed along [010] the structures exhibit similar packing patterns (Figure 4.26). Viewed from this perspective, both structures appear to form quaternary adducts, giving the impression that the two structures are similar.

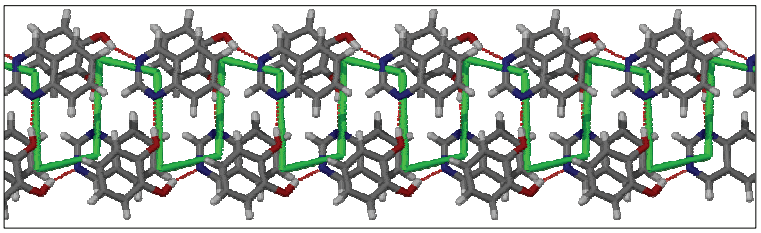

Figure 4.25 A hydrogen bonded tape of O2BN3 showing the stretched out helix. Surrounding molecules have been omitted for clarity.

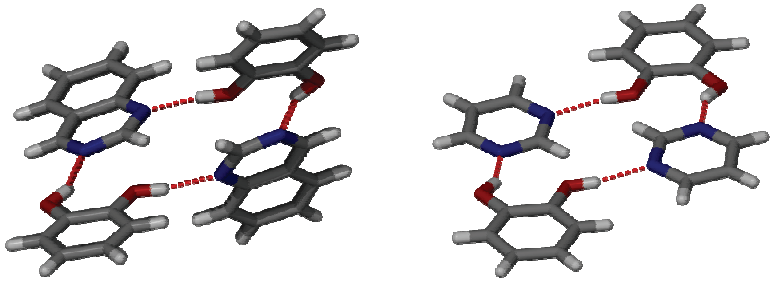

Figure 4.26 The O2BN3 (left) tape, $C_2^2(10)$, showing a packing pattern similar to that of the discrete adduct of O2N3 (right), $R_2^2(18)$.

The 1-D tapes pack along [100] to form an arrangement resembling a sandwich herringbone motif. For the purposes of discussion, the 1-D tapes are bisected longitudinally in the plane of the page such that each tape consists of two strands (grey and blue molecules represent separate strands). Each strand forms a sandwich herringbone motif in a 2-D layer. The 3-D arrangement then consists of two *anti*-parallel herringbone motifs (Figure 4.).

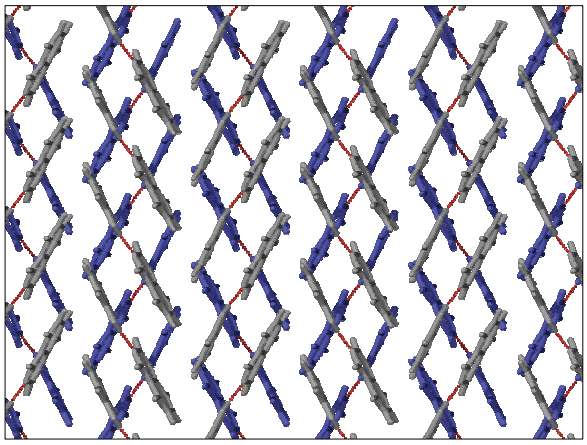

Figure 4.27 Packing diagram of O2BN3 viewed along [100] Two *anti*-parallel herringbone motifs, formed by separate strands of the hydrogen bonded tapes, are shown in blue and grey.

Solvent-drop grinding experiments were once again carried out using three different molar ratios. Two of the experiments yielded solid products, while the third (1:2 molar ratio) yielded an oily product, which could not be subjected to PXRD analysis. However, single-

crystals were obtained from an ethanol solution of the oily product and were analysed by SCD to yield the structure reported here. A simulated PXRD diffractogram of this structure is compared to the PXRD results of the two solid products (Figure 4.28). In this instance, all products are comparable, regardless of the molar ratio used.

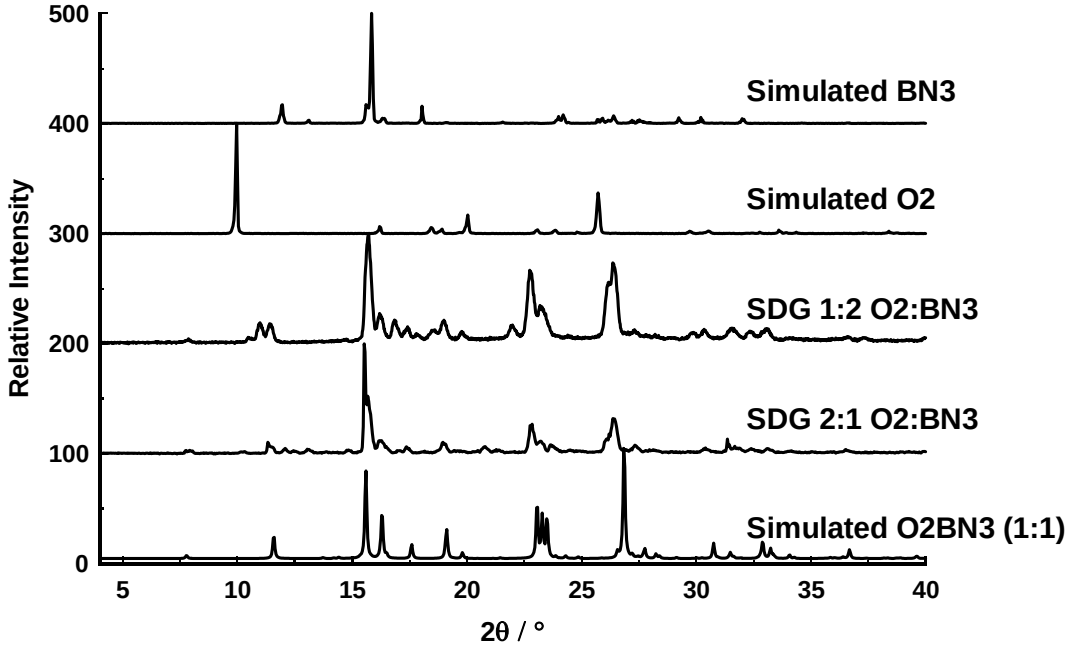

Figure 4.28 PXRD comparison of two SDG experiments utilising different molar ratios with the simulated pattern of O2BN3.

4.2.5 O3BN3 – Resorcinol and Quinazoline

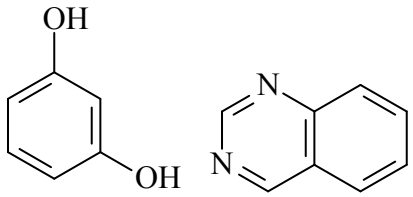

Scheme 4.6 Co-crystal formers resorcinol and quinazoline

Attempts to obtain a crystal structure of O3BN3 have, thus far, been unsuccessful. Solvent-drop grinding experiments prepared from three different molar ratios afforded oils in all cases. Because these cannot be analysed by PXRD, they were dissolved in ethanol and allowed to evaporate slowly in an effort to obtain single-crystals suitable for SCD. Although solid materials were obtained from these crystallisations, they were unsuitable for SCD analysis and the sample quantity was insufficient for PXRD analysis.

Alternative methods (melt crystallisation, seeding, *etc*.) or variations (different solvents, increased grinding time) on current methods are being taken into consideration for further

crystallisations. Interestingly, the problems encountered here were also met in the preparation of the analogous O3N3 system (Chapter 3, section 3.2.5). A method yet to be implemented as part of this study is to seed a solution with a co-crystal composed of similar components. The seed crystal offers a basis on which the components in solution can build. If the two co-crystal structures share similar features, this method may be viable for single-crystal growth of the co-crystals in question.

4.2.6 O4BN3 – Hydroquinone and Quinazoline (1:2 and 2:1 ratios)

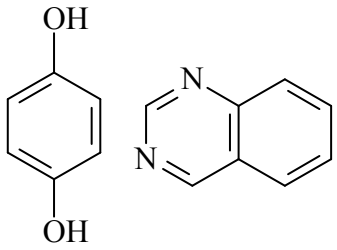

Scheme 4.7 Co-crystal formers hydroquinone and quinazoline

α–O4BN3 (1:2)

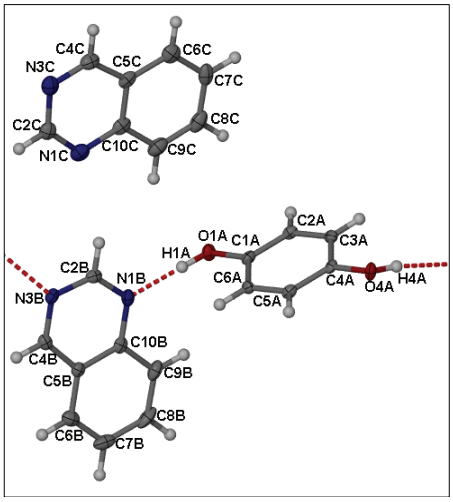

Figure 4.29 A thermal ellipsoid plot of the ASU of *α*–O4BN3 showing a hydrogen bonded chain and a free molecule of quinazoline.

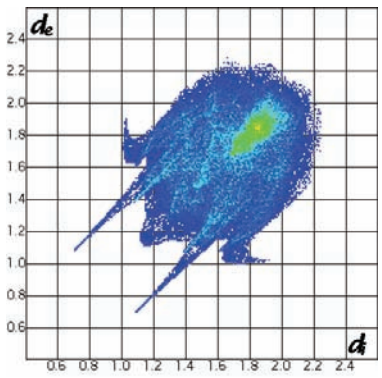

Figure 4.30 Fingerprint plot of *α*–O4BN3

The *α*–form of O4BN3 crystallises in the monoclinic space group, $P2_1/c$. This structure contains two symmetry–independent quinazoline molecules and one hydroquinone molecule in the ASU (Figure 4.29). One quinazoline molecule (**B**) utilises both hydrogen bond acceptors to hydrogen bond with hydroquinone, thus forming 1-D chains, $C_4^4(22)$. The second quinazoline molecule (**C**) is excluded from forming strong hydrogen bonds and appears to fill the spaces created by hydrogen bonded chains. In filling these spaces,

molecule **C** participates in offset π⋯π interactions with two symmetry-independent molecules (**B)** orientated 180° to one other. The π⋯π interactions are clearly visible in the fingerprint plot, Figure 4.30 (green area on diagonal), along with the characteristic wings of C–H⋯π interactions between molecule **B** and the hydroquinone ring of neighbouring chains. The 1-D chains undulate owing to hydroxyl hydrogen atoms orientated in the *trans*–conformation. Hydroquinone and quinazoline molecules in neighbouring chains are positioned approximately perpendicular to one another to facilitate C–H⋯π interactions. This is the first example encountered in this study where one of the component molecules only participates in weak interactions.

Though direct comparison cannot be made with the O4N3 co-crystal (Chapter 3), there are similarities to the co-crystal of *β*–O4N2. If the 'superfluous' quinazoline molecules (**C**) are omitted from a single layer representation of *α*–O4BN3, the molecules form a hydrogen bonded chain. The hydrogen bonded chain of *α*–O4BN3 undulates in a similar fashion to the ternary adducts in *α*–O4N2 (Figure 4.31) and the orientation of the two pyridazine molecules in *α*–O4N2 is similar to that of the 1,3 positioning of the N–atoms in quinazoline. Chains in *α*–O4BN3 are offset in the layer to compensate for the larger dimensions of quinazoline compared to pyridazine and causes undulation of the hydrogen bonded chains to be less pronounced in *α*–O4BN3.

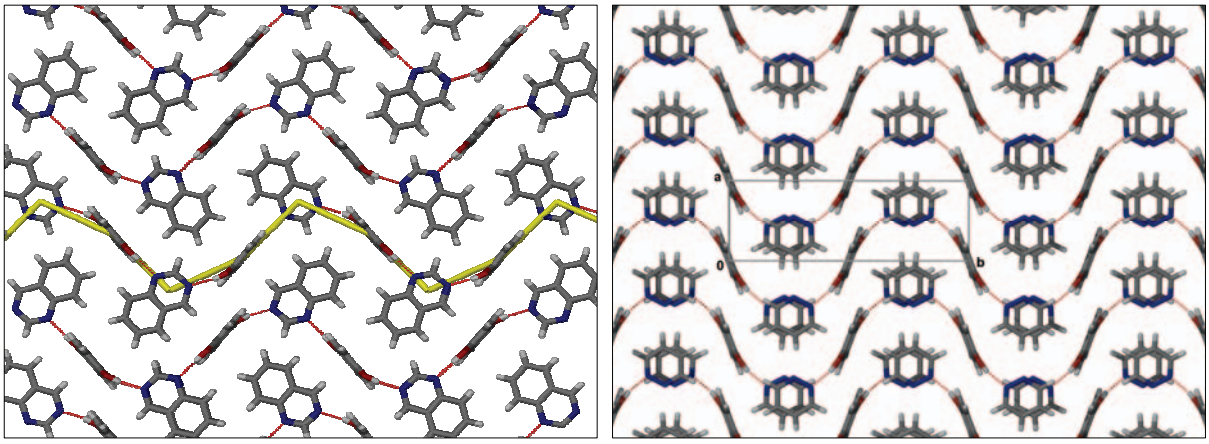

Figure 4.31 Packing diagrams of *α*–O4BN3 (left) and *β*–O4N2 (right). Molecule **C** is omitted from the structure of *α*–O4BN3 to highlight similarities with the structure of *β*–O4N2.

β–O4BN3 (2:1)

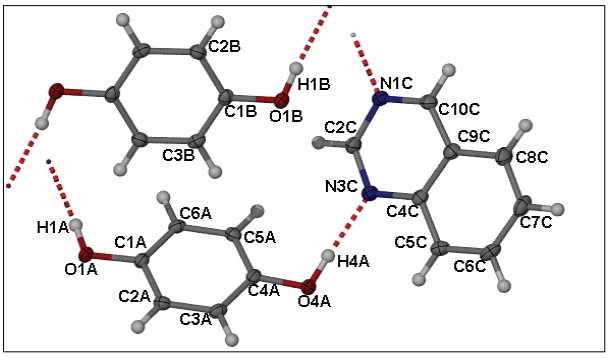

Figure 4.32 Thermal ellipsoid plot showing the ASU of *β*–O4BN3 (only ASU atoms are labelled).

The *β*–form of O4BN3 crystallises in the triclinic space group, $P\bar{1}$, with one and a half molecules of hydroquinone and an entire molecule of quinazoline in the ASU (Figure 4.32). Although there have been examples of different ratios of hydrogen bond donor and acceptor molecules in the co-crystal structures presented thus far, there has not yet been an example of a structure containing hydroquinone in both possible conformations (*cis* and *trans*) within the same crystal. A CSD search revealed that, of the 112 organic structures containing hydroquinone (3-D coordinates determined), only three examples exist that include hydroquinone in both the *cis*- and *trans*-conformations in the same structure (EBIMEI, ISEJIZ, XEZROK). The structure reported here is the only known structure in which the *cis*-conformer forms hydrogen bonded rings with a heteromolecule. Hydroquinone molecules in the *trans* conformation hydrogen bond to the *cis* conformer *via* O–H⋯O interactions to form 2-D tapes, $C_4^4(20)$. Adjacent tapes are kept in close association by C–H⋯O interactions. Alternate layers pack in an offset manner, thus creating an ABAB stacking pattern.

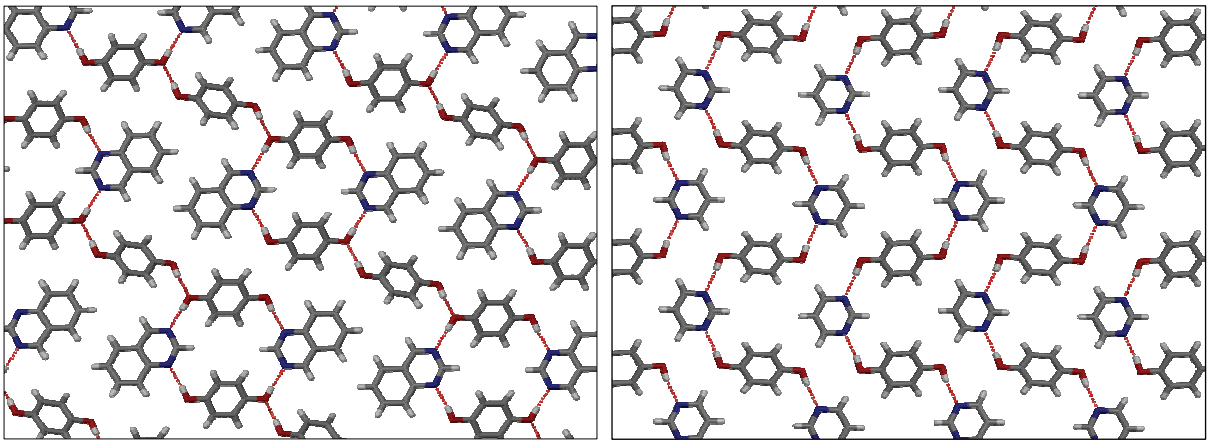

Figure 4.33 A single layer packing diagram of *β*–O4N3 (left) and O4N3 – Scenario 1 (right) showing the similarity between the hydrogen bonded chains in both structures.

Although, the molar ratio of *β*–O4BN3 is different to that of O4N3 (Chapter 3), there exist similarities between the structures. The structure of O4N3 (Chapter 3) presents an interesting phenomenon because of the manner in which molecules are disordered, resulting in two possible hydrogen bonding motifs that cannot be differentiated based solely on SCD analysis. It is, therefore, interesting to consider that both motifs might exist in the structure. The structure of *β*–O4BN3 supports this possibility and can arguably be used in the interpretation of the disorder involved in O4N3. In a single layer of *β*–O4BN3, both hydrogen bonded rings and chains exist in the array (Figure 4.33, left). If the *trans*–conformation hydroquinone molecules are omitted from the structure of *β*–O4BN3 this motif is clearly related to the ring motif possible in the structure of O4N3 (Figure 4.34). The larger quinazoline molecules of *β*–O4BN3 enforce a shift of the rings such that they do not align. This shift provides the space required for the *trans*–hydroquinone to slot into the array.

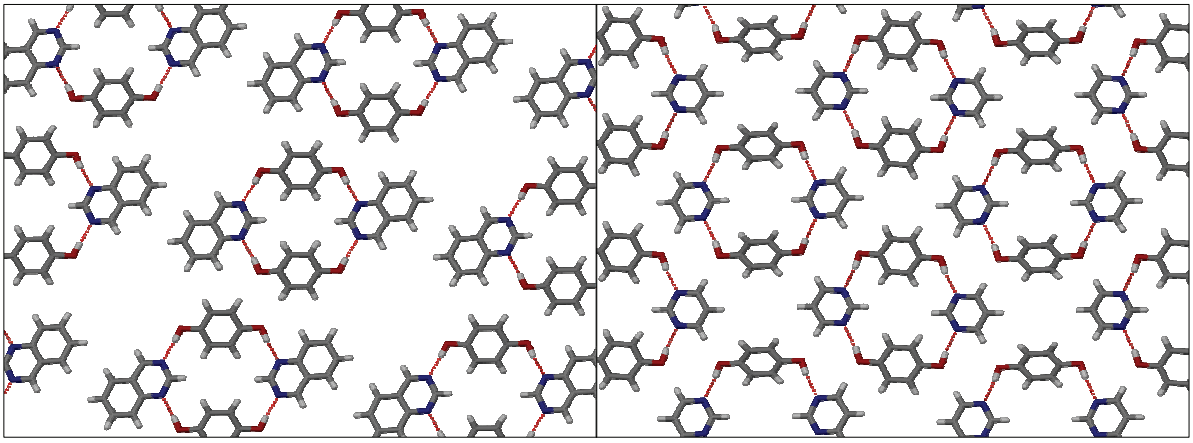

Figure 4.34 A single layer of the packing array of *β*–O4BN3 (left) with *trans*-hydroquinone (molecule **B**) omitted to highlight rings, compared to the hydrogen bonded rings of O4N3, Scenario 2 (right).

Solvent-drop grinding experiments were carried out using three different molar ratios of hydroquinone and quinazoline. The diffractogram simulated by *α*–O4BN3 is comparable to the product resulting from SDG experiment using an excess of quinazoline. The simulated pattern also bears similarities to the equimolar ratio SDG product. The pattern of the third SDG product (2:1) is comparable to that simulated from *β*–O4BN3 data, as well as to that of the equimolar ratio SDG product (Figure 4.35). Therefore, it is assumed that the equimolar product is a mixture of the 1:2 and 2:1 SDG co-crystals.

The DSC traces (Figure 4.36) of the two crystal structures presented here are decidedly different. The *β*–form is more thermally stable, melting at 123 °C whereas the *α*–form melts at 89 °C. The *α*–form apparently converts to the *β*–form during the thermal program of the DSC analysis, with a second thermal event, corresponding to the melt of the *β*–form

observed at approximately 123 °C. This phenomenon has not yet been confirmed by PXRD analysis of the *α*–form at elevated temperatures. Conversion *via* thermal conditions would be an important result, since it shows that the *β*–form can be prepared either by using an excess of hydroquinone or by the conversion of the *α*–form using elevated temperature. The 1:1 SDG product produces a similar trace to that of the *α*–form, with thermal events at T_{on} = 88 °C and 128 °C. This result supports the assumption of a mixture of the 1:2 and 2:1 co-crystals in this product.

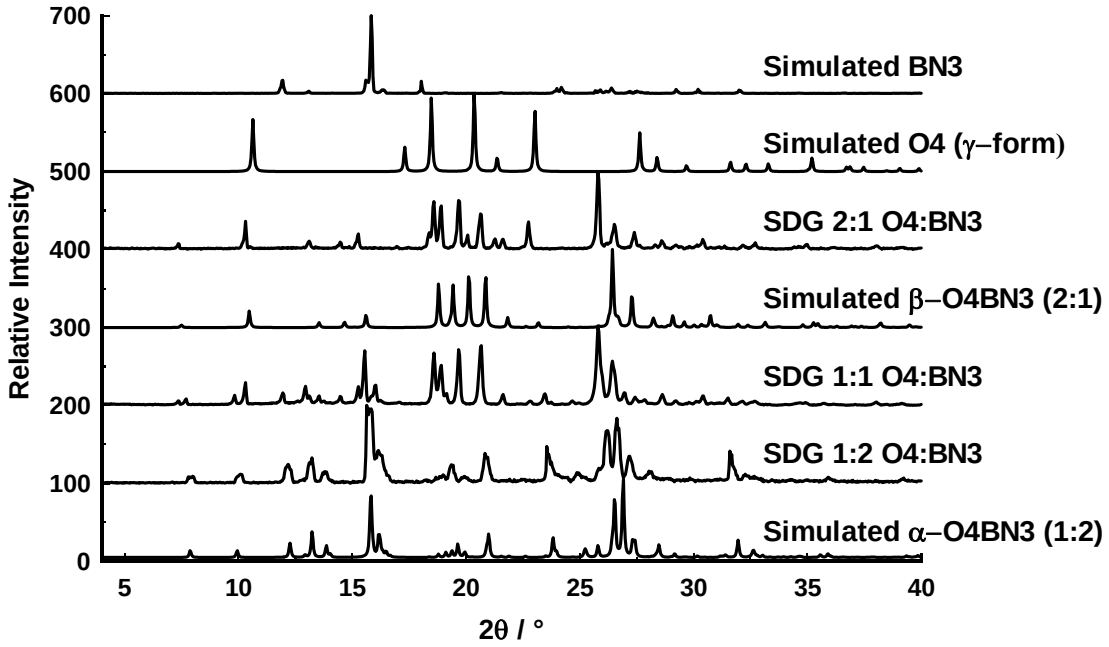

Figure 4.35 Comparison of PXRD results of the three SDG experiments (1:1, 1:2 and 2:1) with the simulated patterns of O4BN3 (α and β) and the pure components, hydroquinone and quinazoline.